

25<sup>th</sup> ABCM International Congress of Mechanical Engineering  
October 20-25, 2019, Uberlândia, MG, Brazil

## Stability Analysis Of Compressible, Binary, Planar Jets Using DNS and LST Methods

**Vinicius Hagemeyer Chiumento**

**Leandro Franco de Souza**

**Josuel Kruppa Rogenski**

Departamento de Matemática Aplicada e Estatística, Instituto de Ciências Matemáticas e de Computação, Universidade de São Paulo  
vinicius.chiumento@usp.br, lefraso@icmc.usp.br, josuelkr@gmail.com

**Marcio Teixeira de Mendonca**

Instituto de Aeronáutica e Espaço, Departamento de Ciências e Tecnologia Aeroespacial, Ministério da Defesa  
marciomtm@fab.mil.br

### **Abstract.**

*A binary jet is a fluid flow of a given chemical species moving with a higher velocity than the surrounding ambient that has another chemical species. Binary flows are very common in combustion systems where a high homogenization of the fluid mixture is desired and the mixing could be enhanced by turbulence. The stability theory analyzes the growth of small disturbances that leads to transition between laminar and turbulent flows. The stability of compressible, binary, planar jets composed by oxygen and hydrogen are analyzed in this study using Direct numerical simulation (DNS) and Linear Stability Theory (LST). The amplification rates obtained by both methods are compared and show good agreement. The varicose and sinuous modes are analyzed and show that the sinuous modes has a higher amplifications rate than the varicose mode.*

**Keywords:** laminar-turbulent transition, direct numerical simulation, compressible jets, binary mixture, linear stability Theory

### **1. INTRODUCTION**

A binary jet is composed of a fluid moving in a higher velocity than the surrounding ambient containing a different fluid. The two fluids may be both gases, which is the case in the present study. The two streams will mix as they flow downstream and disturbances introduced upstream will be dissipated if the flow is stable. If the flow is unstable these disturbances will be amplified. The present study is similar to the studies of Mendonça (2014) and Rogenski *et al.* (2017). Transition to turbulence occurs earlier in flows with a high amplification rate and the turbulent flow will result in a more homogeneous fluid mixtures. This is desired because the efficiency of combustion in propulsive systems is dependent on the mixing between reactants (Na *et al.*, 2006).

There are two stability modes in jet stability, a varicose mode and a sinuous mode. The varicose mode is characterized by a zero normal velocity component at the center line of the jet. The sinuous mode are characterized by the oscillating of perturbations. Two jet flow configurations are studied, the  $H_2 - O_2 - H_2$  jet flow configuration where hydrogen is in the ambient co-flow and oxygen is in the jet stream; and the  $O_2 - H_2 - O_2$  jet flow configuration where oxygen is in the ambient co-flow and hydrogen is in the jet stream.

### **2. FORMULATION AND NUMERICAL METHOD**

Two distinct methods are used in the present study, the linear stability theory (LST), that is based in the Rayleigh equation written in terms of the Gropengiesser variable (Salemi, 2006), and the direct numerical simulation (DNS). The amplification rate as well the eigenfunctions obtained from LST are compared to the results obtained from DNS.

The LST formulation considers the flow decomposed in a base flow and a disturbance. The resulting equations for the disturbances are solved considering normal mode solutions, where the disturbances are treated as waves that propagate downstream. According to Salemi (2006) the Rayleigh equation reduces to

$$(\alpha \bar{u} - \omega) \frac{d\hat{v}}{dy} - \alpha \hat{v} \frac{d\bar{u}}{dy} = \frac{i\alpha^2 G \hat{p}}{\gamma_1 M \alpha_1^2}, \quad (1)$$

and

$$\bar{\rho}i(\alpha\bar{u} - \omega)\bar{v} = -\frac{1}{\gamma_1 Ma_1^2} \frac{d\hat{p}}{dy}. \quad (2)$$

Where  $G$  is

$$G = \frac{1}{\rho} - Ma_1^2 \frac{\gamma_1 (\alpha\bar{u} - \omega)^2}{\gamma \alpha^2}. \quad (3)$$

The Gropengiesser transformation for sinuous mode is presented in Eq. 4. For the varicose mode the inverse Gropengiesser transformation given by eq 5 is used.

$$\chi = \frac{i\alpha\hat{p}}{\gamma_1 Ma_1^2 \hat{v}} \quad (4)$$

$$\chi = \frac{\gamma_1 Ma_1^2 \hat{v}}{i\alpha\hat{p}} \quad (5)$$

Using eq. 4 or 5 in eq. 1 and 2 the system of equations is reduced to only one equation. For the LST, the procedure to solve this equation is summarized by the following algorithm Salemi (2006):

- For a given value of frequency  $\omega$  a value of  $\alpha$  is guessed;
- A 4<sup>th</sup>-order Runge-Kutta method is use to perform two integrations: from the upper and lower boundaries  $y_{\max}$  and  $y_{\min}$  to  $y = 0$ ;
- The solutions of the integrals are compared at  $y = 0$ ;
- If the solutions do not match, a new value of  $\alpha$  is estimated using the secant method.

The Navier-Stokes equations, energy equation and the mass fraction transport equation are written using flux vectors. They are presented in equation 6, where  $\mathbf{Q} = \{\rho, u, v, T, S_1\}$  and  $\mathbf{F}$ ,  $\mathbf{G}$  are flux vectors.

$$\frac{\partial \mathbf{Q}}{\partial t} + \frac{\partial \mathbf{F}}{\partial x} + \frac{\partial \mathbf{G}}{\partial y} = 0 \quad (6)$$

For the DNS simulation, the solution is obtained using high-order compact finite difference schemes to represent spatial derivatives and a 4<sup>th</sup>-order Runge-Kutta method for time integration (Lele, 1992) (Souza *et al.*, 2005). Disturbances are introduced by adding temporal infinitesimal variables to the base-flow profile at the inflow boundary. The disturbances are represented by as a set of eigenfunctions obtained from LST results (Mendonça, 2014). The procedure according to Lacerda (2016) and Mendonça (2014) is:

- Specify initial conditions for  $u$ ,  $v$ ,  $s_1$  and  $T$  in all the numerical domain;
- Calculate  $\rho$ ;
- At each step of the Runge-Kutta method calculate the mass fraction of the mixture, molar fraction of the mixture, the dynamic viscosity of both species, the viscosity of the mixture, thermal conductivity of each specie, the thermal conductivity of the mixture and the right-hand side of the system;
- Update boundary conditions according to eigenfunctions from LST, based on Lacerda (2016) ;
- A high order numerical filter (Lele, 1992) is applied in both directions.

The eigenfunctions from LST are used as boundary condition at the inlet of the DNS domain. The fluctuation is calculated by eq. 7 where  $\phi$  is a generic conserved variable,  $\omega$  is the oscillation frequency and  $t$  is the time.  $|\hat{\phi}|$  is the magnitude of disturbance and  $\Theta_\phi$  is the phase of disturbance.

$$fct_\phi = |\hat{\phi}| \cdot \cos(\Theta_\phi) \cdot \sin(-\omega \cdot t) + fct_u \quad (7)$$

The adopted mesh has 2046 grid points in the main flow direction (x-direction) and 1046 grid points in the normal direction (y- direction). Each simulation is performed using 40 processors with Message Passing Interface (MPI) communication in a computational grid composed by four processors in normal direction and ten in streamwise direction. Near the bottom, upper and outflow boundaries buffer zones were implemented as well as mesh stretching.

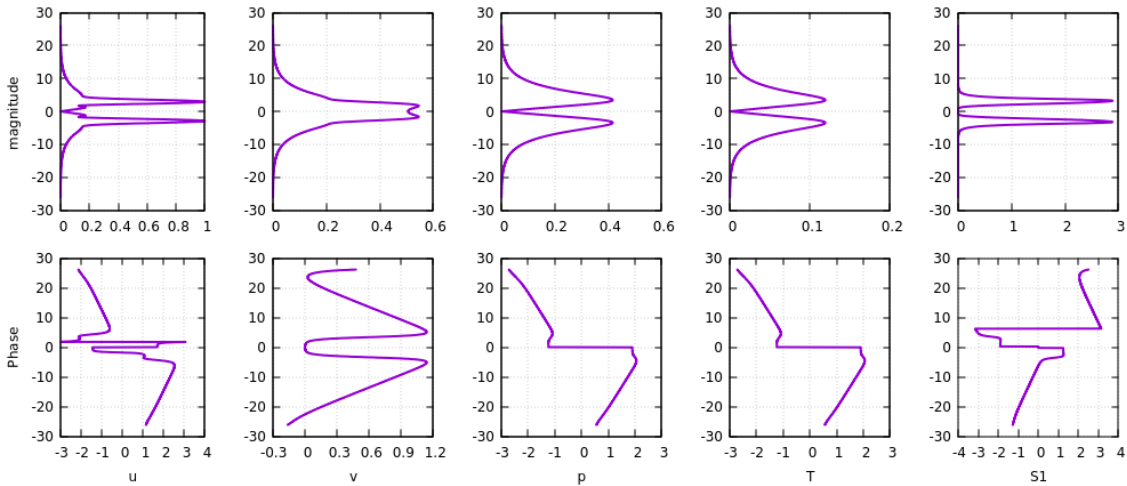


Figure 1. Amplitude and phase distribution for the sinuous mode.

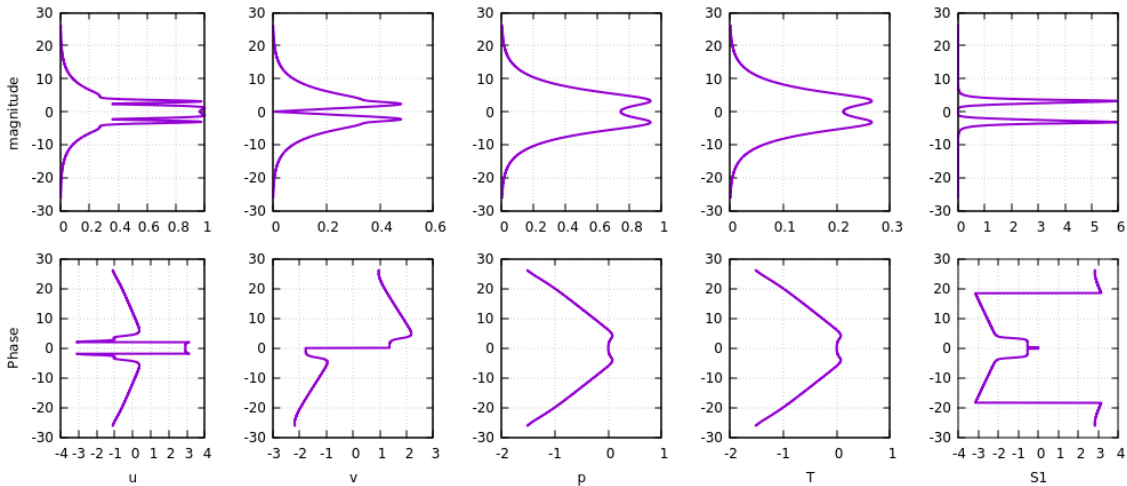


Figure 2. Amplitude and phase distribution for varicose mode.

## 2.1 Eigenfunctions

The base-flow profile is a hyperbolic tangent function described in Eq. 8, where  $y$  is the direction perpendicular to the flow.

$$u_1 = \frac{1}{2} + \frac{1}{2} \tanh \left[ \frac{3}{8} \left( \frac{R}{y} - \frac{y}{R} \right) \right] \quad (8)$$

For each case simulated a disturbance is superposed on the base flow at the inlet and different eigenfunctions are used depending on the case considered. The eigenfunctions for  $\omega = 0.2$  are presented in fig. 2 and 1 for the varicose and sinuous modes respectively.

## 3. RESULTS

The DNS results are analyzed using Fourier transformation along the  $x$  axis, resulting in a curve where it is possible to observe three regions in the flow: numerical receptivity, linear and nonlinear regimes. A regression is made using the data in the linear region resulting in the amplification rate for the DNS simulation, in the same figure, it is provided  $H_2$  concentration values. Figure 3 shows the concentration of  $H_2$  in a section of DNS domain for the sinuous mode. The black line is the amplitude of oscillation obtained from the Fourier analysis, one can see that the linear region is between  $x = 36$  and  $x = 334$ .

Figure 4 shows the amplification rate  $\alpha_i$  as a function of oscillation frequency  $\omega$  for two different configurations: (a)  $H_2 - O_2 - H_2$  jet flow configuration when hydrogen is in the co-flow and oxygen is in the jet; (b)  $O_2 - H_2 - O_2$  jet flow configuration when hydrogen is in the jet and Oxygen is in the co-flow. The maximum amplification rate for the  $H_2 - O_2 - H_2$  jet is  $\alpha_i = 4.4216e - 2$  at  $\omega = 0.3847$  for sinuous mode. For the varicose mode the maximum

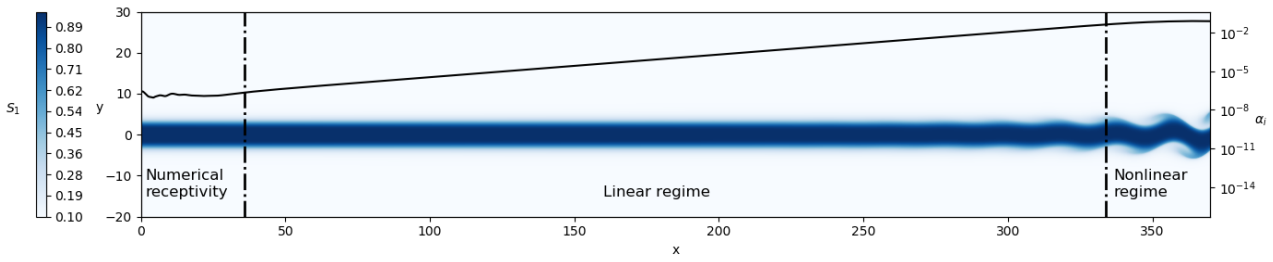


Figure 3.  $H_2$  concentration contours for the  $O_2 - H_2 - O_2$  jet,  $\omega = 0.2$ ,  $M = 1.25$  and disturbance amplitude growth given by a Fourier analysis.

amplification rate is  $\alpha_i = 3.1711e - 2$  at  $\omega = 0.4826$ . For the  $O_2 - H_2 - O_2$  configuration the maximum amplification rate is  $\alpha_i = 4.0896e - 2$  at  $\omega = 0.2267$  for the sinuose mode, and  $\alpha_i = 3.2367e - 2$  at  $\omega = 0.21$  for the varicose mode. The  $H_2 - O_2 - H_2$  jet is unstable for a larger frequency range than  $O_2 - H_2 - O_2$  jet. Using  $M = 1.5$  the behavior of the flow is very similar to the behavior using  $M = 1.5$ , beside this, the amplification rate for  $M = 1.5$  is smaller than the amplification rate for  $M = 1.25$ .

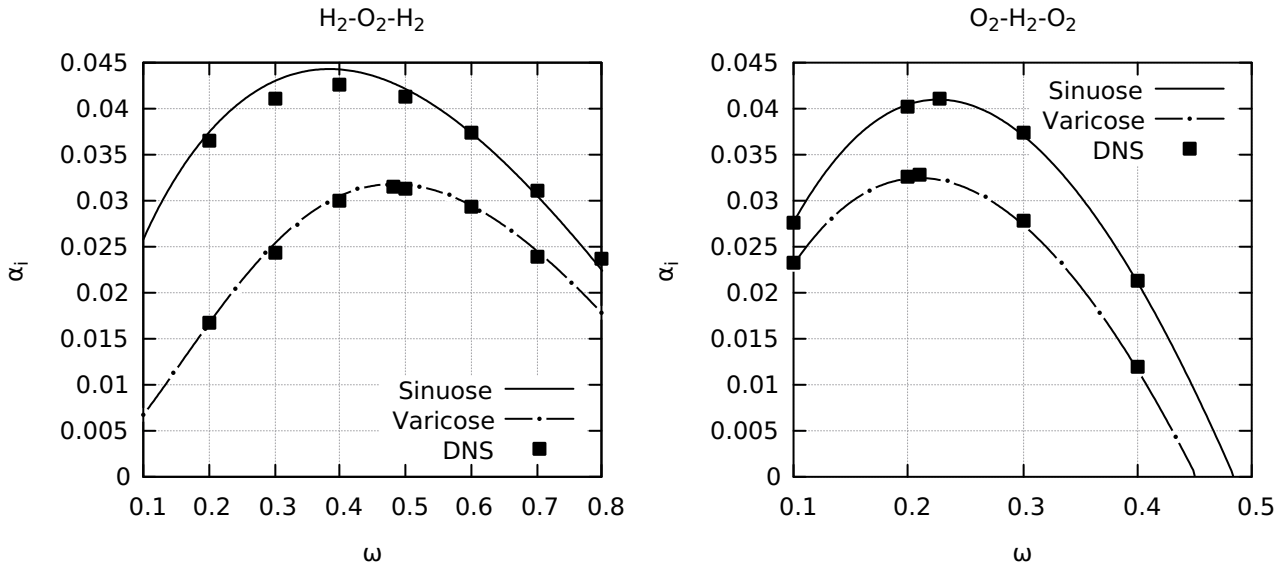


Figure 4. Amplification rate ( $\alpha_i$ ) as a function of oscillation frequency ( $\omega$ ) for both jet configurations using Mach = 1.25. At left the jet configuration is  $H_2 - O_2 - H_2$  and the configuration on the right is  $O_2 - H_2 - O_2$ . The lines show the results obtained by LST and the dots are the results from DNS.

In sinuose mode the superior and inferior vortices are formed alternating in  $x$  position, furthermore for the varicose mode the upper vortices em the bottom vortices are formed along side. Figure 6 shows the density contours for the sinuose mode, for this simulation  $\omega = 0.2$  and  $M = 1.25$ . In this figure is possible to see the alternating vortices. The vortices formed by varicose mode could be observed in fig. 7, that shows the density contours for the varicose mode, for this simulation  $\omega = 0.2$  and  $M = 1.25$ , in this case the velocity component in  $v$  at the center line is zero.

#### 4. CONCLUSION

The DNS and LST methods show a good agreement. For all the cases simulated, the varicose mode showed lower amplification rates than sinuose mode. The  $O_2 - H_2 - O_2$  jet configuration is more stable than the  $H_2 - O_2 - H_2$  jet configuration, furthermore for low values of  $\omega$  the amplification rate of  $O_2 - H_2 - O_2$  jet configuration is higher than the amplification rate of  $H_2 - O_2 - H_2$  jet configuration. The results also show that the compressibility causes a stabilizing effect on the flow. This behavior has been perceived by Papamoschou and Roshko (1988) for a plane shear layer.

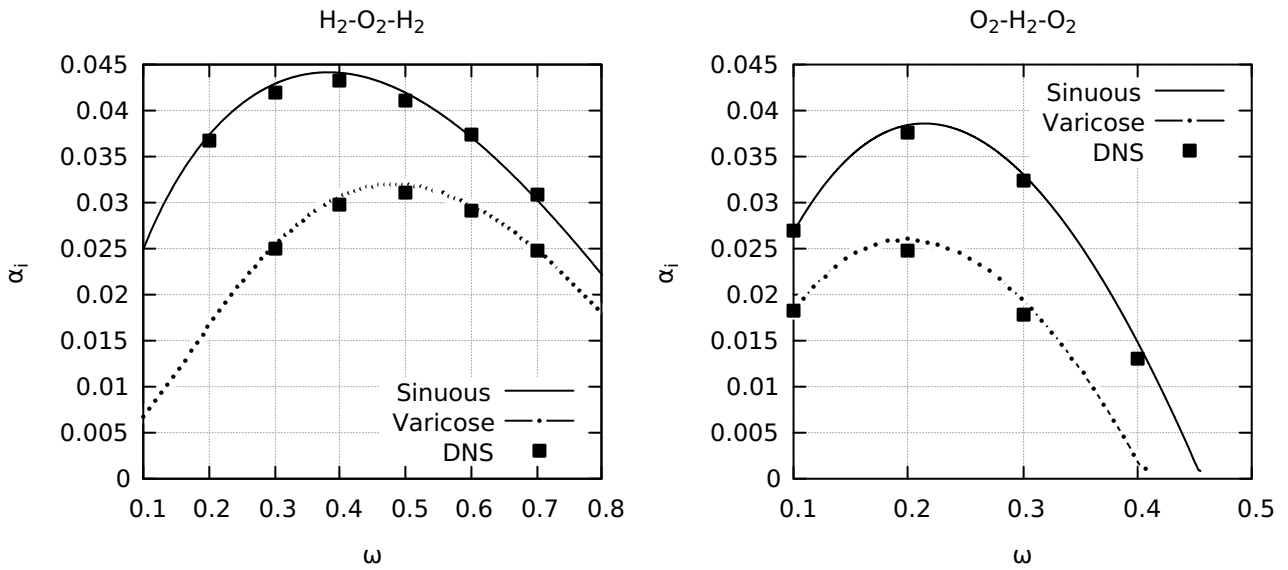


Figure 5. Amplification rate ( $\alpha_i$ ) as a function of oscillation frequency ( $\omega$ ) for both jet configurations using Mach = 1.5. At left the jet configuration is  $H_2 - O_2 - H_2$  and the configuration on the right is  $O_2 - H_2 - O_2$ . The lines show the results obtained by LST and the dots are the results from DNS.

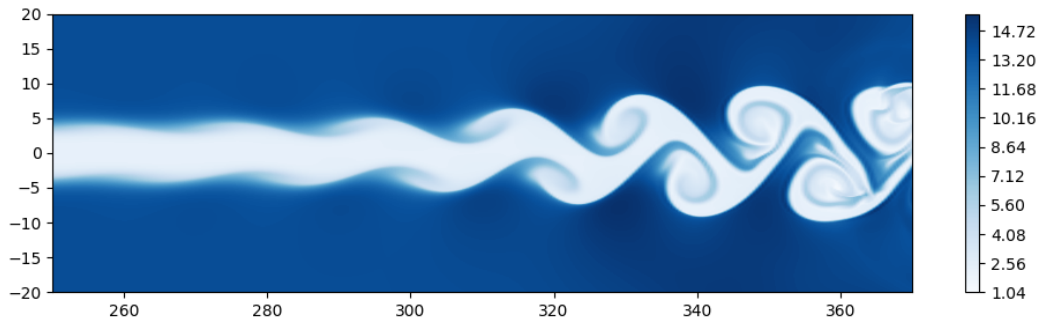


Figure 6. density contours for the  $O_2 - H_2 - O_2$  jet,  $\omega = 0.2$ ,  $M = 1.25$  for sinuous mode.

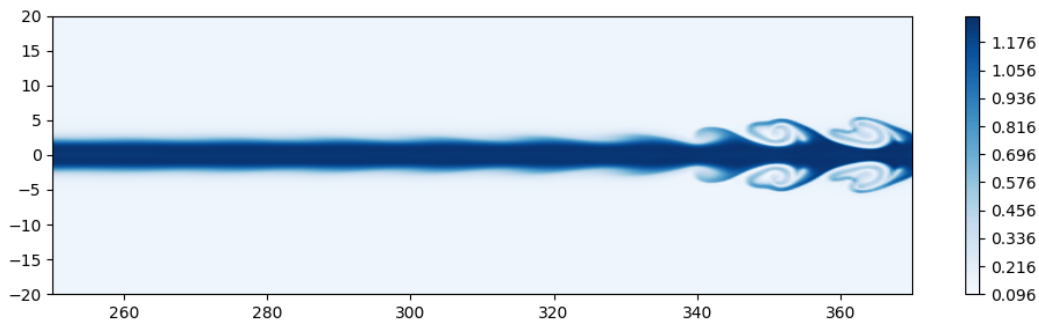


Figure 7. density contours for the  $H_2 - O_2 - H_2$  jet,  $\omega = 0.4$ ,  $M = 1.25$  for varicose mode.

## 5. ACKNOWLEDGEMENTS

The authors thank CNPq and FAPESP for financial support and ICMC-USP for technical support and infrastructure. Research carried out using the computational resources of the Center for Mathematical Applied to Industry (CeMEAI) funded by FAPESP (Process Number 2013/07375-0).

## 6. REFERENCES

- Lacerda, J.F., 2016. *Aeroacústica computacional através de simulação numérica direta de escoamentos livres cisalhantes compressíveis*. Ph.D. thesis, Universidade de São Paulo.
- Lele, S.K., 1992. "Compact finite difference schemes with spectral-like resolution". *Journal of computational physics*, Vol. 103, No. 1, pp. 16–42.
- Mendonça, M.T., 2014. "Linear stability analysis of binary compressible mixing layers modified by a jet or a wake deficit". In *52nd Aerospace Sciences Meeting*. p. 1444.
- Na, Y., Lee, S. and Shin, D., 2006. "Linear stability analysis of the reacting shear flow". *Journal of Mechanical Science and Technology*, Vol. 20, No. 8, p. 1309.
- Papamoschou, D. and Roshko, A., 1988. "The compressible turbulent shear layer: an experimental study". *Journal of fluid Mechanics*, Vol. 197, pp. 453–477.
- Rogenski, J.K., Souza, L.F., Mendonça, M.T. and Morris, P.J., 2017. "Growth of even and odd instability modes in compressible binary jet flows". In *24th ABCM International Congress of Mechanical Engineering*.
- Salemi, L.D.C., 2006. *Análise de estabilidade linear de camada de mistura laminar compressível binária*. Master's thesis, Instituto Nacional De Pesquisas Espaciais, Cachoeira Paulista.
- Souza, L.F., Mendonça, M.T. and Medeiros, M.A.F., 2005. "The advantages of using high-order finite differences schemes in laminar–turbulent transition studies". *International journal for numerical methods in fluids*, Vol. 48, No. 5, pp. 565–582.